

Rotational bands and surface waves in α - ^{40}Ca elastic scattering

R. Fioravanti

Consiglio Nazionale delle Ricerche, C.N.R. Genova, Italy

G. A. Viano

Dipartimento di Fisica dell'Università di Genova, Istituto Nazionale di Fisica Nucleare-Sezione di Genova, Italy

(Received 10 July 1996; revised manuscript received 21 November 1996)

The scattering of heavy ions gives clear evidence of resonances which may be grouped in families like the rotational bands. The classical Breit-Wigner theory makes use of fixed poles which describe locally the resonances, but the global character of the rotational sequences is completely lost. Furthermore, the phenomenology shows that the rotational sequences evolve into surface waves. Again the classical Breit-Wigner theory, in view of its local character, cannot describe this evolution. In this paper we describe the resonances by the use of poles of the scattering amplitude in the complex angular-momentum plane: moving poles. However, in order to interpolate a sequence of resonances belonging to the same family we must add to the poles a term which takes into account the repulsive forces due to the Pauli principle and to the hard core. This term describes the downward crossing, through $\pi/2$, of the phase shifts after each resonance. At higher energies the effect of the exchange forces tends to vanish and simultaneously the resonances evolve towards diffractive effects: we have the surface waves creeping around the target. This phenomenon is described in our theory by the moving poles as the imaginary part of the angular momentum increases for increasing energy. Besides a detailed study of this theory we present here an extensive analysis of the α - ^{40}Ca elastic scattering which gives clear phenomenological support to the model. [S0556-2813(97)02204-8]

PACS number(s): 25.70.Ef, 24.10.Ht, 25.55.-e

I. INTRODUCTION

In the classical theory of resonances in nuclear physics (Breit-Wigner theory) each resonance is described by a fixed pole (Breit-Wigner pole) and accordingly we have only a local description of the phenomenon: i.e., in the neighborhood of the energy position of the resonance. On the other hand, the phenomenology of ion collisions, and even the hadron interactions, give clear evidence of bands of resonances which should be regarded as a global phenomenon. As a typical example one could keep in mind the rotational bands in α -nuclei elastic scattering. We can remark, indeed, that in the classical theory of resonances the properties of analyticity of the scattering amplitude are not related to the symmetry properties involved in nuclear models. Analogously the classical theory, in view of the fact that it gives only a local description of the phenomenon, is unable to describe the evolution from quantum-mechanical to semiclassical phenomena. Returning once more to the example of α -nuclei elastic scattering, the experimental data show that the widths of the resonances increase with increasing energy and the rotational resonances evolve smoothly into surface waves creeping around the target. This evolution is not described in the classical theory.

In order to connect dynamics with symmetry in the case of rotational bands, the singularities of the scattering amplitude should be located in the complex plane of the angular momentum. In spite of a large number of papers devoted to the analytical properties of the scattering amplitude, the various applications related to the extension of the angular momentum to complex values remain disconnected and sometimes rather obscure. The method originated long ago in connection with the diffraction of radio waves around the

earth (see [1]). It was then reconsidered by Levy-Keller and others [2,3] and applied to the so-called "geometrical-diffraction theory." Successively Regge [4] proved certain analyticity properties of the scattering amplitude in the complex angular-momentum plane for the class of Yukawian potentials. Starting from these results the Regge representation was then widely used to derive asymptotic behaviors of the cross sections for high values of the energy.

Here we rather turn our attention to the applications which were, in a certain sense, at the origin of the method: the diffraction. More precisely we describe, at first, the elastic resonances as poles of the scattering amplitude in the complex angular-momentum plane in the sense of Regge. But we will show that if we really want to connect various resonances, belonging to the same family, with a pole trajectory, then we must take into account the effect of the echoes of the resonances: the downward crossing of the phase shifts across $\pi/2$, after a resonance (see [5]). As we shall show the echoes, in these nuclear collisions, are essentially due to the effects of the exchange and of the hard-core forces. We must then modify the representation formula of the phase shifts (obtained by projecting on the partial waves the complex angular-momentum pole representation of the scattering amplitude) adding a term which takes into account the repulsive forces due to the Pauli exchange effects and to the hard-core forces. All these questions will be treated in two subsections of Sec. II. As the energy increases we pass from a quantum-mechanical to a semiclassical description of the interaction, and the effect of the exchange forces tends to vanish. Simultaneously the resonances evolve into surface waves. We have the diffractive effects which can be properly described by the use of the classical methods originally introduced by Watson and Sommerfeld [1] for studying the diffraction of radio

waves around the earth. We can then describe the smooth evolution of resonances into surface waves. These questions will be analyzed in the third subsection of Sec. II.

The phenomenology will be illustrated in Sec. III analyzing the elastic scattering of α particles by ^{40}Ca . Finally, let us mention that one of us has already analyzed, in two previous papers [6,7], the rotational sequence of resonances in the α - α elastic scattering [6] and the resonances in the π^+ - p elastic collision [7], working with methods based on the ideas illustrated above. Here we extend and complete the theory; furthermore, the analysis of α - ^{40}Ca scattering shows very clearly two trajectories of opposite signature, interpolating one the rotational resonances of even parity, the other those of odd parity, which at higher energy, where the semi-classical approximation holds true, evolve into surface waves creeping around the target.

II. THEORY

A. Complex angular-momentum picture of a resonance in a Yukawian potential model

If the potential $V(r)$ belongs to the Yukawian class, then the scattering amplitude $f(E, \theta)$ (where E is the energy and θ is the scattering angle in the center-of-mass system) can be represented as follows (Regge representation):

$$f(E, \theta) = \frac{i}{2} \int_{-1/2-i\infty}^{-1/2+i\infty} \frac{(2\lambda+1)f_\lambda(E)P_\lambda(-\cos\theta)}{\sin\pi\lambda} d\lambda + \sum_{n=1}^N \frac{g_n(E)P_{\lambda_n}(-\cos\theta)}{\sin\pi\lambda_n}. \quad (1)$$

Here we denote by λ the extension of the angular momentum l to complex values and accordingly $\lambda_n(E) = \alpha_n(E) + i\beta_n(E)$ give the locations of the poles of the partial scattering amplitudes analytically continued in the complex half-plane $\text{Re}\lambda > -1/2$, while $g_n(E)$ are the residues of these poles and $P_\lambda(-\cos\theta)$ denote the Legendre functions. The first term on the rhs of formula (1) is called the ‘‘background integral.’’ The second term is a sum over a finite number of poles which all lie in the first quadrant of the complex λ plane.

Let us, now, suppose that at a certain energy and for a specific value of n , $\alpha_n \equiv \text{Re}\lambda_n$ crosses an integer, while $\beta_n \equiv \text{Im}\lambda_n$ is positive but much less than unity (i.e., $0 < \beta_n \ll 1$); then the corresponding term in the sum over poles becomes very large: we have a pole dominance. However, in view of the fact that $P_\lambda(-\cos\theta)$ presents a logarithmic singularity at $\theta=0$ (see [1]), the pole approximation cannot represent the amplitude forwards. At $\theta=0$ it is indeed necessary to take into account the contribution of the background integral in order to make the amplitude $f(E, \theta)$ finite and regular. On the contrary the pole approximation is worth trying backwards, where the background integral receives much less contribution since $(\sin\pi\lambda)^{-1}$ acts as a powerful cutoff for high values of $|\lambda|$ while $P_\lambda(-\cos\theta)$ is finite. In conclusion the following one-pole approximation can be used for describing the scattering amplitude backwards in the neighborhood of a sharp and isolated resonance:

$$f(E, \theta) \approx g(E) \frac{P_{\lambda(E)}(-\cos\theta)}{\sin\pi\lambda(E)} \quad (2)$$

(where the index n is superfluous and it has been omitted).

From formula (2) one can derive a picture of the resonance in the complex angular-momentum plane, which differs in a significant way from the classical one associated with the Breit-Wigner formalism. In this latter theory the exponential decay law of the resonance is associated with the width of the resonance which is related to the imaginary part of the location of the pole (Breit-Wigner pole) in the k plane. Returning to our formalism let us note that the Legendre function $P_\lambda(-\cos\theta)$ ($\lambda \in C$) corresponds to nonunitary representations of the rotation group. Here the nonunitarity of the rotation group describes the breaking of the angular symmetry of the resonance, due to the fact that the resonance is not stable, and accordingly we do not have angular isotropy except in the case of collision of identical particles (this case will be discussed below). We are thus naturally led to introduce a ‘‘spin-width’’ proper of the resonance. The ‘‘spin width’’ tends to zero as the lifetime of the resonance tends to infinity and therefore the angular asymmetry proper of the resonance tends to vanish. It is, indeed, zero for the bound states.

Let us note that even if the scattering amplitude given by the approximation (2) diverges for $\theta=0$, nevertheless the total cross section derived from formula (2) is finite; indeed we have

$$\sigma_{\text{tot}} = \frac{H(E)}{|\sin\pi\lambda(E)|^2}, \quad (3a)$$

$$H(E) = 2\pi |g(E)|^2 \int_0^\pi |P_\lambda(-\cos\theta)|^2 \sin\theta d\theta, \quad (3b)$$

and the integral on the rhs of formula (3b) converges in view of the fact that the singularity of $P_\lambda(-\cos\theta)$ at $\theta=0$ is logarithmic.

Let us now project the amplitude (2) on the l th partial wave obtaining

$$f_l = \frac{e^{2i\delta_l} - 1}{2ik} \approx \frac{g}{\pi} \frac{1}{(\alpha + i\beta - l)(\alpha + i\beta + l + 1)}, \quad (4)$$

where δ_l denotes the l th phase shift.

Next, when the elastic unitarity condition may be applied, the following relationship among g , α , and β can be derived:

$$g = -\frac{\pi}{k} \beta(2\alpha + 1) \quad (5)$$

and finally we obtain the following approximation for the l th phase-shift δ_l :

$$\delta_l \approx \sin^{-1} \frac{\beta(2\alpha + 1)}{\{[(l-\alpha)^2 + \beta^2][(l+\alpha+1)^2 + \beta^2]\}^{1/2}}. \quad (6)$$

Let us note that approximation (6) does not satisfy the asymptotic behavior proper of Yukawian phase shifts: i.e., an exponential decrease in l of the terms δ_l . This means that approximation (6) is faithful for low values of l only. This

defect, however, is not very serious at low energy where a few terms of the partial-wave expansion are sufficient to describe the scattering amplitude. The advantages of a representation like that given by formula (6) is due to the fact that (i) at fixed energy it gives several phase shifts at different values of l , with an acceptable approximation for small values of l ; (ii) α depends on the energy E [i.e., we have the pole trajectory $\alpha(E)$]; when $\alpha(E)$ equals the integer l (the orbital angular momentum) and β is very small, we have $\sin\delta_l \approx 1$, i.e., we have a resonance. Therefore, formula (6) can describe, in principle, a sequence of resonances in the various partial waves. In our case the possibility of connecting several resonances with a pole trajectory [as illustrated in point (ii)] deserves particular interest. But in order to guarantee that this connection really works, we must have more information on the behavior of the pole trajectory itself.

From the standard theory of Regge poles, we obtain the following relationship:

$$\frac{\beta}{d\alpha/dE} = \frac{\Gamma}{2}, \quad (7)$$

where Γ is the width of the resonance. If $d\alpha/dE$ is positive, then Γ is positive since the poles lie in the first quadrant of the complex λ plane and β is positive. In such a case we can associate with Γ a lifetime $\tau = 1/\Gamma$ ($\hbar = 1$), and we can speak of a physical resonance because the outgoing flux of particles is delayed with respect to the incoming flux: τ can be interpreted as a time delay. It has been proved, however, that the trajectories $\alpha(E)$ produced by Yukawian potentials turn back towards the left half-plane [4]. When $\alpha(E)$ turning back crosses an integer, then $d\alpha/dE$ is negative and Γ is negative too in view of the fact that β is positive. Since Γ is negative, one cannot associate this phenomenon with a resonance and a time delay, but rather it corresponds to the downward passage of the phaseshift through $\pi/2$: we have an ‘‘echo’’ (see [5]) of the resonance. At this point we meet a drastic difficulty if we pretend connecting several resonances (like those encountered in α - ^{40}Ca system) by using approximation (2) [or equivalently Eq. (6)] without adding any other term. In fact, the phase shifts describing these interactions present ordered sequences of resonances and echoes (see the section devoted to the phenomenological analysis): any phase shift after a resonance presents the corresponding echo. Now if we consider a pole trajectory derived from approximation (2) [or Eq. (6)] it could not connect two or more resonances, because after a first crossing of $\alpha(E)$ through an integer corresponding to the angular momentum of a resonance ($d\alpha/dE$ positive), the pole trajectory will rapidly turn back to reach the same integer, with negative derivative, in order to describe the corresponding echo. Otherwise if one supposes that a pole trajectory connects several resonances in an ordered sequence, then this trajectory, turning to the left, cannot reproduce in order the sequence of the echoes. But this fact is not surprising if we think that the nuclear interactions cannot certainly be explained simply in terms of Yukawian potentials. We must take into account the exchange effects due to Pauli exclusion principle as well as the hard-core forces. The next subsection is precisely devoted to these questions.

B. Hard-core forces and echoes of resonances

There is clear phenomenological evidence that in the collision of ions the downward passage of the phaseshift through $\pi/2$ is related to the repulsive forces due to the Pauli exclusion principle and to the hard core. In particular, in the α - α elastic scattering a pure nonlocal potential, which represents all the effects of antisymmetrization and exchange of the nuclear interactions, is insufficient to reproduce the echoes and a repulsive hard core must be added in order to reproduce the experimental data (see [8]).

Let us then consider some properties of the phase shifts produced by a pure hard-core potential. We recall, first of all, that the S function derived from the scattering by an impenetrable sphere of radius r_0 reads (see [9]):

$$S(\lambda, k) = -\frac{H_{\lambda+1/2}^{(2)}(kr_0)}{H_{\lambda+1/2}^{(1)}(kr_0)}, \quad (8)$$

where $H_{\lambda+1/2}^{(1),(2)}(kr_0)$ are the Hankel functions of first and second kind, respectively. By the use of the following decomposition of the Hankel functions into Bessel and Neumann functions,

$$H_{\lambda+1/2}^{(1),(2)}(kr_0) = J_{\lambda+1/2}(kr_0) \pm iN_{\lambda+1/2}(kr_0) \quad (9)$$

[(+) refers to the first kind and (−) to the second kind of Hankel function] and recalling that $S(\lambda, k) = e^{2i\delta(\lambda, k)}$, we obtain

$$\delta(\lambda, k) = \tan^{-1} \frac{J_{\lambda+1/2}(kr_0)}{N_{\lambda+1/2}(kr_0)}, \quad (10)$$

where $J_{\lambda+1/2}(kr_0)$ are the Bessel and $N_{\lambda+1/2}(kr_0)$ are the Neumann functions. Then from the asymptotic behavior of the Neumann functions, for large values of k , we deduce that the zeros of $N_{\lambda+1/2}(kr_0)$ are located approximately at

$$\lambda = \frac{2}{\pi} kr_0 - (2n + 1) \quad (n = 0, 1, 2, \dots) \quad (11)$$

and all lie on the real axis of the λ plane (for real values of k). The echoes correspond to the zeros of $N_{\lambda+1/2}(kr_0)$. Indeed using for the Bessel functions $J_{\lambda+1/2}(kr_0)$ an asymptotic expression analogous to that used for the Neumann functions $N_{\lambda+1/2}(kr_0)$ we obtain the following behavior of the phase shifts for large values of k :

$$\delta(\lambda, k) = -kr_0 + \lambda \frac{\pi}{2}. \quad (12)$$

Therefore when λ attains the values (11), we have $\delta(\lambda, k) = -\pi/2 \pmod{\pi}$; accordingly $\sin^2\delta(\lambda, k) = 1$ and the cross section shows peaks which are not resonances, but echoes, since the phase shifts are decreasing. If we consider integer values of λ , corresponding to physical phase shifts and we put $kr_0 = [\alpha(\alpha + 1)]^{1/2}$, then formula (10) reads as follows:

$$\delta_l(k) = \tan^{-1} \frac{J_{l+1/2}\{\alpha(\alpha+1)\}^{1/2}}{N_{l+1/2}\{\alpha(\alpha+1)\}^{1/2}} \quad (13)$$

and it describes a sequence of echoes in the various partial waves, as

$$[\alpha(\alpha+1)]^{1/2} = [l+(2n+1)] \frac{\pi}{2} \quad (l, n = 0, 1, 2, \dots). \quad (14)$$

It is very difficult and probably impossible to determine exactly the shape of the potential responsible of the interaction of ions, nevertheless one may reasonably assume of knowing the behavior of $V(r)$ for r large enough (let us say the “asymptotic behavior”) and the behavior of the potential near the origin. The former is related to the range of the nuclear forces and one can assume that the potential presents a Yukawian tail. The latter is related to the repulsive character of the nuclear forces at short distance and to the effects of the Pauli exclusion principle. One is therefore tempted to assume a hard-core repulsive potential close to the origin, let us say for $r \leq r_0$, and then for large r a Yukawian type potential. As far as we know there does not exist a rigorous mathematical theory of the scattering from a potential of this type. The only results obtained (see [10]) are essentially numerical and concern a potential of the following form:

$$V(r) = \begin{cases} \infty & (0 \leq r \leq r_0), \\ \int_{\mu_0}^{+\infty} \sigma(\mu) \frac{e^{-\mu r}}{r} d\mu & (r > r_0). \end{cases} \quad (15a) \quad (15b)$$

The authors [10] show that we may still speak of poles of the scattering amplitude in the complex angular-momentum plane and of pole trajectories. Furthermore, the trajectories are unbounded or approach a finite limit point, but in either case remain only in one half-plane. In view of these considerations and of the arguments, which shall be illustrated below, we simply glue together the approximation (6) and formula (14) obtaining

$$\delta_l(k) \approx \sin^{-1} \left(\frac{\beta(2\alpha+1)}{\{[(l-\alpha)^2 + \beta^2][(l+\alpha+1)^2 + \beta^2]\}^{1/2}} \right) + A(k) \tan^{-1} \frac{J_{l+1/2}\{\alpha(\alpha+1)\}^{1/2}}{N_{l+1/2}\{\alpha(\alpha+1)\}^{1/2}}. \quad (16)$$

Let us note that in formula (16) the first term is dominant in the neighborhood of an isolated and sharp resonance, for $\alpha \approx l$; and in this region the second term is negligible. On the contrary, the second term is dominant in the neighborhood of an echo, where the first one tends to vanish. The behavior of formula (16) corresponds precisely to the physical mechanism of the resonance and of the echo. The first one is produced at small values of k and for large r : the particle is trapped for a while by the effective potential, and accordingly we observe a peak in the cross section due to the fact that $\sin^2 \delta_l \approx 1$ (i.e. δ_l is crossing $\pi/2$ with positive derivative). For increasing values of k , when $\alpha \approx (l+1)\pi/2$, we have an echo in the l th partial wave due to the fact that the l th phase shift is now passing downward across $\pi/2$. This echo is due to the repulsive forces (Pauli exchange and hard-core forces), which are, in the present simplified scheme, represented by the hard-core forces only. Since the exchange forces are a pure quantum-mechanical effect and tend to vanish at the classical limit, the parameter A , in formula (16), is not a constant, but decreases with energy. The transition from quantum to semiclassical behavior is precisely given by the dependence on the energy of β and A : β is an increasing function of E ($E = k^2$), while A is a decreasing function of E . In conclusion formula (16) may describe a band of resonances and echoes in the various partial waves.

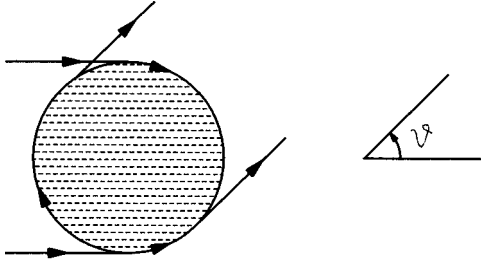
Let us now suppose that the colliding particles are identical bosons: this is the case of α - α scattering. In this situation the collision will be described by the even partial waves only, and accordingly we shall observe a rotational band of resonances with even parity and angular momentum: 0^+ , 2^+ , 4^+ . In this case the scattering amplitude must be symmetrized and the representation of the phase shifts (16) must be modified accordingly, i.e.,

$$\delta_l(k) \approx \sin^{-1} \left(\frac{1+(-1)^l}{2} \frac{\beta(2\alpha+1)}{\{[(l-\alpha)^2 + \beta^2][(l+\alpha+1)^2 + \beta^2]\}^{1/2}} \right) + A(k) \tan^{-1} \left(\frac{1+(-1)^l}{2} \frac{J_{l+1/2}\{\alpha(\alpha+1)\}^{1/2}}{N_{l+1/2}\{\alpha(\alpha+1)\}^{1/2}} \right). \quad (17)$$

Remark: Let us note that in this case the symmetrization of the scattering amplitude requires the introduction, in approximation (2), of a Legendre function of the type $P_\lambda(\cos\theta)$ [in addition to $P_\lambda(-\cos\theta)$]. Then the approximation will fail not only forwards, but also backwards, because we will have a logarithmic singularity not only at $\theta=0$, but also at $\theta=\pi$.

Analogously if the colliding particles are fermions, the scattering amplitude must be antisymmetrized, and the collision will be described by the odd partial waves only. Then the representation of the phase shifts must be written as follows:

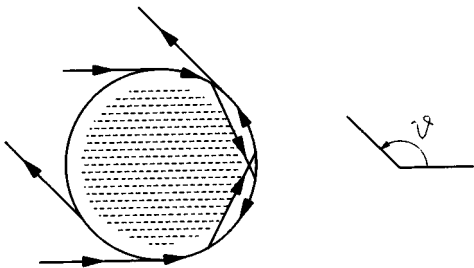
$$\delta_l(k) \approx \sin^{-1} \left(\frac{1-(-1)^l}{2} \frac{\beta(2\alpha+1)}{\{[(l-\alpha)^2 + \beta^2][(l+\alpha+1)^2 + \beta^2]\}^{1/2}} \right) + A(k) \tan^{-1} \left(\frac{1-(-1)^l}{2} \frac{J_{l+1/2}\{\alpha(\alpha+1)\}^{1/2}}{N_{l+1/2}\{\alpha(\alpha+1)\}^{1/2}} \right). \quad (18)$$

FIG. 1. Diffracted rays emerging in direction θ .

Even if the colliding particles are distinguishable, as in the case of the α - ^{40}Ca collision, nevertheless the presence of exchange forces can clearly separate the even from the odd partial-wave amplitudes: the even cannot be interpolated with the odd. We are then forced to fit the even phase shifts with formula (17), and the odd phase shifts with formula (18) (see the next section devoted to the phenomenological analysis).

C. Surface wave theory and diffractive scattering

When the energy increases, inelastic and reaction channels open, and the elastic unitarity condition does not hold true; accordingly the potential acquires an imaginary part. As we have seen in the previous subsection the effect of the exchange forces tends to vanish as we pass from a quantum-mechanical to a semiclassical description of the collision; accordingly $A(k)$ tends to zero for increasing values of $E = k^2$. On the other hand, β is an increasing function of the energy and therefore, even if $\alpha(E)$ goes through an integer value, nevertheless we do not observe sharp peaks in the cross section since $|\sin\pi(\alpha + i\beta)|^{-1} \approx e^{-\pi\beta}$. We have a transition from sharp resonances to diffractive surface effects, which we want to illustrate in this subsection. Let us note that while the sharp resonances involve essentially only one partial wave, on the contrary the diffractive surface effects involve a certain packet of partial waves and consequently there is a mixing of even and odd waves. We are then forced to return to approximation (2) of the scattering amplitude, rather than to the approximation representing the phase shifts δ_l . Now we try a picture of the physical process as it is described by approximation (2). With this in mind we represent the interaction region as a sphere weakly absorbing at the center and with a thin transparent layer at the border. The width of this transparent layer will reduce as the incident energy increases and it will tend to zero at the high-energy limit (see Figs. 1 and 2). The assumption of a relatively weak absorption is very important as it will be clarified in the next

FIG. 2. Diffracted rays emerging in direction θ after a shortcut.

section. Then we evaluate the contribution of those diffracted rays which describe an arc of geodesic around the obstacle or turn around the sphere a certain number of times and emerge in a certain direction θ . Here we suppose that the mass of the incident particles is much less than the mass of the target; then the massive scatterer suffers little recoil and acts practically as a fixed center of mass. Therefore, the c.m. scattering angle and the laboratory scattering angle can be taken equal within a good approximation.

Let us now rewrite approximation (2) in the following form:

$$f(E, \theta) \approx -g(E) \frac{P_{\lambda'-1/2}(-\cos\theta)}{\cos\pi\lambda'}, \quad (19)$$

where we have put $\lambda' = \lambda + 1/2$. Then we introduce the asymptotic behavior of the Legendre function $P_{\lambda'-1/2}(-\cos\theta)$ for $|\lambda'| \rightarrow \infty$, and $|\lambda'|(\pi - \theta) \gg 1$ (see [11]):

$$P_{\lambda'-1/2}(-\cos\theta) \approx \frac{e^{-i[\lambda'(\pi-\theta)-\pi/4]} + e^{i[\lambda'(\pi-\theta)-\pi/4]}}{\sqrt{2\pi\lambda'\sin\theta}} \quad (0 < \theta < \pi). \quad (20)$$

Next we use the following relationship:

$$\frac{1}{\cos\pi\lambda'} = 2e^{i\pi\lambda'} \sum_{m=0}^{\infty} (-1)^m e^{i2\pi m\lambda'} \quad (\text{Im}\lambda' > 0). \quad (21)$$

Therefore we obtain

$$\begin{aligned} \frac{P_{\lambda'-1/2}(-\cos\theta)}{\cos\pi\lambda'} &\approx 2e^{i\pi/4} \sum_{m=0}^{\infty} (-1)^m e^{i2\pi m\lambda'} \\ &\quad \times \frac{e^{i\lambda'\theta} - ie^{i\lambda'(2\pi-\theta)}}{\sqrt{2\pi\lambda'\sin\theta}}. \end{aligned} \quad (22)$$

We are thus led to consider the following series:

$$\begin{aligned} &\sum_{m=0}^{\infty} (-1)^m e^{i2\pi m\lambda'} \frac{e^{i\lambda'\theta} - ie^{i\lambda'(2\pi-\theta)}}{\sqrt{\sin\theta}} \\ &\approx \sqrt{\frac{\pi\lambda'}{2}} e^{-i\pi/4} \frac{P_{\lambda'-1/2}(-\cos\theta)}{\cos\pi\lambda'} \quad (0 < \theta < \pi). \end{aligned} \quad (23)$$

The scattering angle $\theta(0 < \theta < \pi)$ is related to the surface angles $\theta_{0,m}^{\pm}$ in the following way:

$$\theta_{0,m}^+ = \theta + 2\pi m, \quad (24a)$$

$$\theta_{0,m}^- = 2\pi - \theta + 2\pi m \quad (m = 0, 1, 2, \dots), \quad (24b)$$

where $\theta_{0,m}^+$ refer to the counterclockwise traveling rays, while $\theta_{0,m}^-$ refer to the clockwise ones (see Fig. 1). Then in view of formulas (24a) and (24b), the lhs of formula (23) reads

$$\sum_{m=0}^{\infty} (-1)^m \frac{e^{i\lambda' \theta_{0,m}^{\pm}}}{\sqrt{\sin \theta_{0,m}^{\pm}}} \approx g'(\lambda') \frac{P_{\lambda'-1/2}(-\cos \theta)}{\cos \pi \lambda'} \quad (25)$$

[where $g'(\lambda') = \sqrt{\pi \lambda' / 2} e^{-i\pi/4}$]. If in formula (25) we put $kR = \text{Re} \lambda'$, then the terms $e^{i\lambda' \theta_{0,m}^{\pm}}$ represent waves traveling (counterclockwise and clockwise) along geodesics bending the target. The imaginary part of λ' gives the damping factor of these surface waves. Recalling that $\lambda' = \lambda + 1/2$, we get $kR = \text{Re} \lambda + 1/2$ in agreement with the semiclassical approximation which replaces the term $l(l+1)$ with $(l+1/2)^2$. The physical meaning of the factor $(-1)^m$ derives from the fact that at each complete tour around the sphere, the ray crosses two times the symmetry axis of the obstacle which is the caustic (see below). As is well known in optics, and it has been mathematically proved in semiclassical mechanics, each time the trajectory crosses the caustic, the phase changes by a factor $e^{-i\nu\pi/2}$; ν is called the Morse index and it can be evaluated by the methods of differential geometry (see [12]). In our case $\nu=1$, and then at each complete tour we have a factor -1 . It remains to consider the term $(\sin \theta_{0,m}^{\pm})^{-1/2}$. The physical interpretation of this factor is more transparent if we look at the corresponding term $(\sin \theta)^{-1/2}$ in the lhs of formula (23). This term becomes infinity for $\theta=0$ and $\theta=\pi$: i.e., along the symmetry axis of the target. This is the caustic where the geometrical optic approximation becomes infinity and fails.

Let us now return to approximation (2), which we rewrite as follows:

$$f(E, \theta) \approx G^{(0)}(E) P_{\lambda}(-\cos \theta), \quad (26)$$

where $G^{(0)}(E) = g(E) / \sin \pi \lambda(E)$. As we said in the first subsection, $P_{\lambda}(-\cos \theta)$ presents a logarithmic singularity at $\theta=0$ and therefore approximation (26) fails forwards. At $\theta=0$ we have the so-called ‘‘diffraction peak’’ which is, indeed, produced by the interference of the diffracted rays with the other geometrical contributions which can be represented by a term like the background integral. Let us recall, in fact, that the singularity of $P_{\lambda}(-\cos \theta)$, at $\theta=0$, is compensated by the contribution of the background integral. On the contrary, at $\theta=\pi$, $P_{\lambda}(-\cos \theta)$ is equal to 1 and then we have

$$f(E, \pi) \approx G^{(0)}(E) = \frac{g(E)}{\sin \pi \lambda(E)} \approx g(E) e^{-\pi \beta} \quad (27)$$

which can be interpreted as an asymptotic limit satisfied only for high values of the energy. Indeed, at lower energy, we observe the so-called ‘‘ALAS’’ effect (see [12]): anomalously large-angle scattering peak, which is in apparent contradiction with formula (27). The ALAS effect can be explained by the transparent border of the target. In fact, in view of this transparent shell, some of the grazing rays may be refracted and penetrate the peripheral corona. Some of them can take one or more shortcuts and reemerge (see Fig. 2). According to this model approximation (27) should then be modified, and we have $f(E, \pi) \approx \sum_{p=0}^n G^{(p)}(E)$, where $G^{(p)}(E)$ corresponds to the contributions of the rays which have taken p shortcuts in the peripheral shell. In fact it is possible to prove that, if we evaluate the contributions of those diffracted rays which take one or several shortcuts, the

angular distribution is still described, in the first approximation, by the Legendre function $P_{\lambda}(-\cos \theta)$, provided that we limit to consider a sufficiently backward angular region. Therefore the interference effect of the various terms $G^{(p)}$ at $\theta=\pi$ gives rise to the anomalously large backward peaks. As the energy increases the width of the peripheral border decreases and the amplitude $f(E, \pi)$ tends to the asymptotic limit (27).

III. PHENOMENOLOGICAL ANALYSIS

A. Resonances

We test our theory on the α - ^{40}Ca elastic scattering. The reason for this choice is due to the fact that, in this case, the phenomenology presents very clear evidence of rotational bands of resonances which then evolve, at higher energies, into anomalously large backward peaks. In particular, the backangle anomaly is most pronounced for target nuclei with a shell closure (see [13]).

Langanke [13] has calculated the α - ^{40}Ca phase shifts by the use of the resonating-group method. As one can easily observe, looking at the results of [13], the even phase shifts cannot be mixed with the odd ones at low energy. We are then forced to fit the even phase shifts with formula (17), and the odd ones with formula (18). Since the resonances of the system α - ^{40}Ca form rotational bands, then $\alpha(E)$ must satisfy the following equation:

$$\alpha(\alpha+1) = 2IE + C, \quad (28)$$

where $I = \mu R^2$ is the moment of inertia of the system, μ being the reduced mass; I and C can then be determined through the fitting.

Remark: In the previous section we have put $\hbar = 2\mu = 1$, and accordingly we had $k^2 = E$; in this section it is more convenient to use a slightly different system of units keeping $\hbar = c = 1$, while 2μ is not put equal to 1. Consequently in the present section we have $k = (2\mu E)^{1/2}$.

We do not know exactly the dependence of β on the energy. Calculations performed in the potential model (see [14]) indicate, however, that $\beta(E)$ has a slow increase (less than linear) in the region of surface waves. Since we want to see if it is possible to connect resonances with surface waves we shall try a fit taking for β a dependence on the energy of square-root type (exactly as in the case of α - α elastic scattering, see [6]); i.e.,

$$\beta(E) = \gamma(E)^{1/2}, \quad (29)$$

where γ is regarded as a fitting parameter. Finally, for what concerns the coefficient A in formulas (17) and (18), it could be taken constant in the first approximation. But in order to reproduce more faithfully the trend of the phase shifts, in their downward passage through $\pi/2$, we prefer to take for A a Gaussian dependence on l of the following type:

$$A = A_0 e^{-al^2} \quad (A_0, a \text{ constants}). \quad (30)$$

The fits are shown in Fig. 3 and 4.

Remark: In [13] the phase shifts are normalized according to the Swan generalization of the Levinson theorem for redundant states. Here we return to the Levinson theorem in its

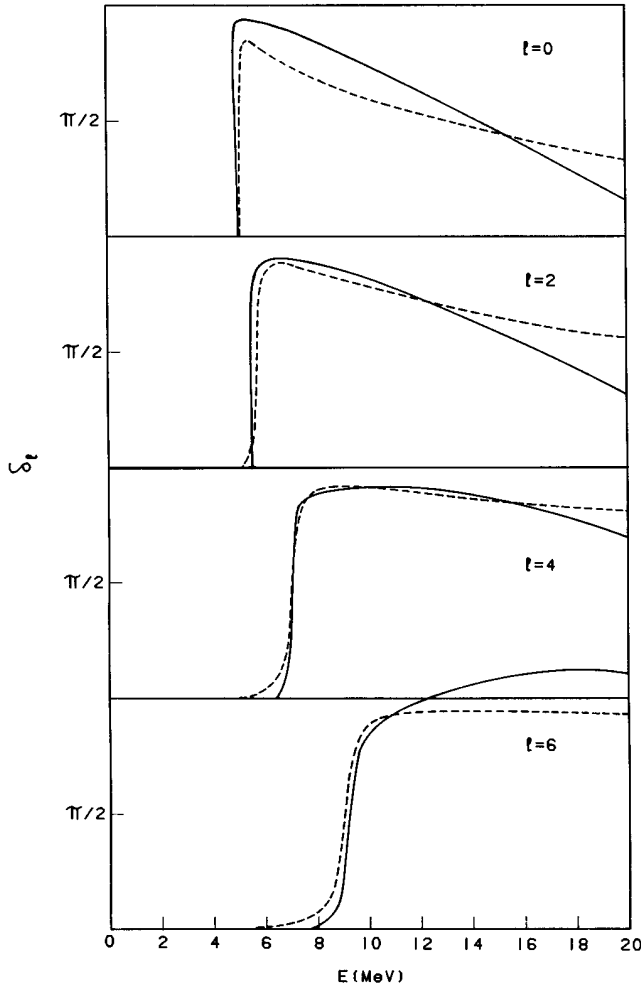


FIG. 3. Phase shifts with even l . The continuous lines represent the phase shifts calculated in [13]; the dotted lines represent the fits.

original formulation: the redundant states with negative energy are to be counted, the ones with positive energy are resonances and do not contribute. The values of the fitting parameters are (a) for l even

$$I = 5.5 \text{ (MeV)}^{-1}, \quad C = -57,$$

$$\gamma = 0.08 \text{ (MeV)}^{-1/2}, \quad A_0 = 0.16, \quad a = 0.05,$$

(b) for l odd

$$I = 5.01 \text{ (MeV)}^{-1}, \quad C = -55,$$

$$\gamma = 0.1 \text{ (MeV)}^{-1/2}, \quad A_0 = 0.26, \quad a = 0.015.$$

From the values of I and C we can then determine the energy positions of the resonances by the use of formula (28). Next by taking the derivative of both sides of Eq. (28), we obtain $d\alpha/dE = 2I/(2\alpha+1)$, and substituting this expression in formula (7) we finally get

$$\Gamma = \frac{\beta(E)(2\alpha+1)}{I} = \gamma \frac{(2\alpha+1)\sqrt{E}}{I}, \quad (31)$$

where in the second equality relationship (29) has been used. Formula (31) gives the energy dependence of the widths of

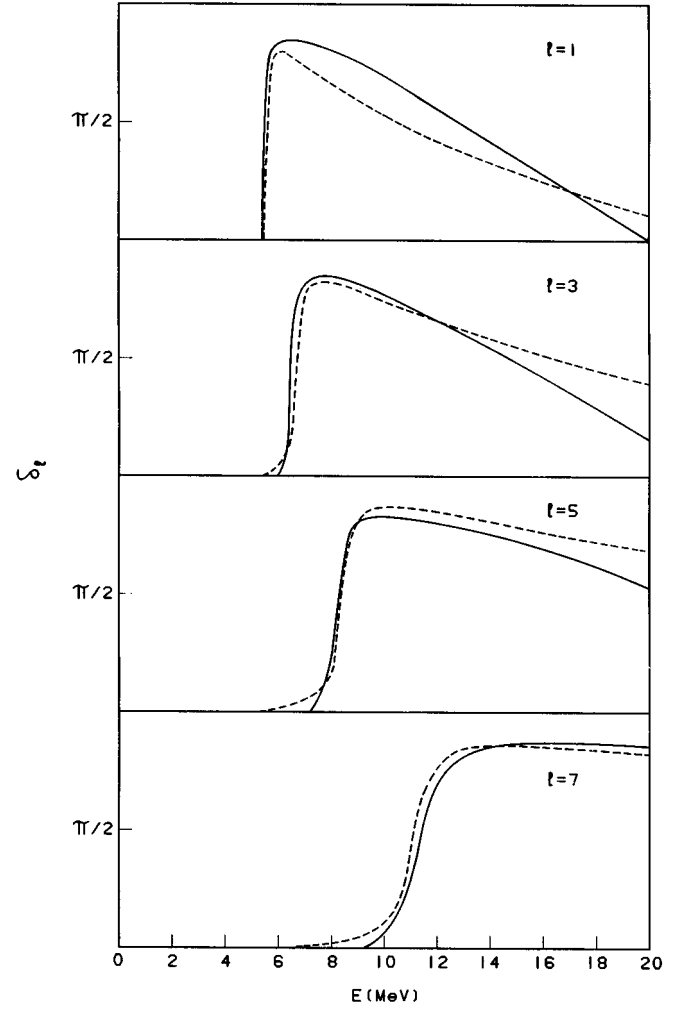


FIG. 4. Phase shifts with odd l . The continuous lines represent the phase shifts calculated in [13]; the dotted lines represent the fits.

the rotational bands. The energy positions and the widths of the resonances [the former obtained by the use of formula (28), the latter by the use of formula (31)] are reported in Tables I and II (for even l values and odd l values, respectively), where they are compared with the corresponding values given in [13].

Remark: In Figs. 3 and 4 the fit of the phase shifts is limited to the values of l between 0 and 6 for l even and between 1 and 7 for l odd. This is motivated by the fact that starting from $l=8$ (for the even l values) and $l=9$ (for the odd l values) the downward trend of the phase shifts, after

TABLE I. The energy positions and the widths of the resonances with even angular momentum. The resonance energies are given in MeV, the resonance widths are given in keV.

l	E_l	Γ_l	E_l	Γ_l
	Present work	Present work	[13]	[13]
0	5.18	32	5.09	70
2	5.72	173	5.69	120
4	7	345	7.09	260
6	9	565	9.48	480
8	11.72	843	12.64	600

TABLE II. The energy positions and the widths of the resonances with odd angular momentum. The resonance energies are given in MeV, the resonance widths are given in keV.

l	E_l Present work	Γ_l Present work	E_l [13]	Γ_l [13]
1	5.7	143	5.6	190
3	6.7	362	6.6	320
5	8.5	641	8.6	640
7	11.1	999	11.5	1150
9	14.5	1446	15.53	1700
11	18.7	1987	20.64	1900

the resonance, is completely missing. This is due to the fact that in this energy region we are rather close to the transition between resonances and surface waves. But still we have resonances belonging to rotational bands. For this reason we still report in Tables I and II the values of E_l and Γ_l (for $l=8$ and $l=9, 11$, respectively) obtained by the use of formulas (28) and (31). Let us, in fact, remark that in order to obtain the energy positions and the widths of the resonances only three fitting parameters (i.e., I , C , γ) are sufficient.

The agreement between our values of the positions and of the widths of the resonances with those given by [13] is satisfactory especially in the case of odd l values. We have, indeed, two distinct rotational bands, one interpolating the resonances with even angular momentum, the other interpolating the resonances with odd angular momentum. Finally from the values of the moment of inertia I , we can derive a value of R ; we obtain: $R=7.8$ fm from the fitting of the phase shifts with even angular momentum, and $R=7.3$ fm from the fitting of the phase shifts with odd angular momentum.

B. Surface waves

As the energy increases the effect of the echoes tends to vanish and accordingly the phase shifts do not present the standard downward trend, in particular the downward passage across $\pi/2$. Simultaneously the widths of the resonances increase, as prescribed by formula (31): the resonances evolve into surface effects. While the sharp resonances are properly described in terms of phase shifts, since each one of them is precisely due to the dominance of one phase shift; the surface effects involve several partial waves. Therefore, rather than use formulas (17) and (18), we must try a fit of the differential cross section by taking the square of the modulus of the rhs of formula (26). Obviously the scattering amplitude cannot be described exclusively in terms of surface waves, neglecting all the others contributions. Therefore, let us return once more to the description of the various processes involved in the collision. Passing from a quantum mechanical to a semiclassical description of the interaction, we can use the Hamilton-Jacobi formalism and introduce various classes of trajectories. We consider, first, the trajectory of a charge Z_1e under the action of the sole Coulomb field of a pointlike charge Z_2e . It is straightforward to derive, in the framework of the Hamilton-Jacobi theory, the expression of the apsidal distance from the origin. We can compare this distance, denoted hereafter by ρ , with the radius R of the

interaction region, which is here pictured as a sphere weakly absorbing at the center and with a thin transparent border [see Sec. II C; for what concerns the sharp edge of the interaction region see remark (i) in the next subsection]. Then ρ can be larger, equal to, or smaller than R . Accordingly we have three classes of trajectories (see also [15]): (i) the trajectories which correspond to those angular momenta such that $\rho > R$, they are determined by the action of the sole Coulomb field, and can be called ‘‘Coulomb trajectories’’; (ii) the trajectories which correspond to $\rho = R$, they may undergo diffraction and will be called ‘‘grazing trajectories’’; (iii) the trajectories which correspond to $\rho < R$, they are reflected or refracted at the surface of the nuclear-interaction sphere.

Let us start by considering the trajectories belonging to classes (ii) and (iii) neglecting, for the moment, the Coulomb effects. In particular, we focus our attention on the refracted trajectories, which play a very important role in the α - ^{40}Ca elastic scattering. In view of the fact that the absorption is relatively weak (even at the center of the interaction region) the trajectories with $\rho < R$, after a refraction at the surface, can penetrate the target and thereafter they may be deflected by nuclear forces: the attractive nuclear force produces a nuclear deflection for small angular momenta [12]. When the modulus of the classical deflection angle has a maximum, as a function of the angular momentum, the cross section presents a singularity due to the fact that many angular momenta are focused to almost the same scattering angle: we have the phenomenon of nuclear rainbow [12]. The maximum modulus of the deflection angle will be called ‘‘rainbow angle’’ and denoted by θ_R . For deflection angles whose modulus is larger than θ_R , no classical trajectory (within the class of refracted trajectories) is possible; however, we may still have complex-valued trajectories (i.e., complex rays). Accordingly the differential cross section decreases exponentially for scattering angles larger than the rainbow scattering angle. Therefore if we limit ourselves to consider the extremely backward angular region, beyond the rainbow scattering angle, we can neglect the contribution of the refracted rays. We have, however, discussed at length the refracted trajectories in view of the fact that the α - ^{40}Ca elastic scattering, because of the weak absorption, provides one of the clearest examples available in nuclear physics of nuclear rainbows, as it has been remarked by McVoy and collaborators who have devoted to this problem and its interpretation three very interesting papers [16–18]. We shall return to this point in the next subsection. In addition to the refracted rays we also have to consider the reflected ones. We shall call ‘‘geometrical component’’ the set of trajectories composed by the union of the reflected and the refracted rays.

Let us, now, focus our attention on the ‘‘grazing trajectories.’’ These may simply describe an arc of geodesic around the target or, being refracted, penetrate the interaction region. Concerning these latter we may assume that the main contribution backwards is due to those rays which, being critically refracted, penetrate the widespread gallery formed by the thin transparent layer at the border of the sphere (see Fig. 2). These rays take one or more shortcuts and emerge backwards. The others entering in the core of the interaction region are partially absorbed (even in the assumption of weak absorption) and their contribution backwards can be ne-

glected. The mechanism of the shortcut is necessary in order to explain the anomalously large backward peaks in the elastic-scattering cross sections; otherwise the exponential damping along the surface is too large to allow a strong enhancement at large angles. The existence of shortcuts is strictly related to the opaqueness of the target; this latter is determined by the number of open channels. The isotope effect in ALAS can then be explained by admitting the existence of shortcuts for closed-shell nuclei and their attenuation, for a larger opaqueness when one considers the isotopes. Analogously the opaqueness increases toward larger energies, and this could explain the fact that the anomalously backward peaks tend to become normal for greater values of the energy. We can then conclude that the grazing trajectories give rise to the surface waves.

These surface waves interfere with the geometrical component. In particular, we recall once more that the function $P_\lambda(-\cos\theta)$ presents a logarithmic singularity at $\theta=0$, whereas the scattering amplitude is finite. In a potential model this singularity is compensated by the contribution of the background integral (see the previous section). This compensation can be interpreted, from a physical viewpoint, as the interference between surface waves and the geometrical component which produces the forward “diffraction peak.” Let us, however, note that this interference is not only relevant forwards but in a large angular range. But we have already observed that the real-valued refracted rays do not emerge in an angular region beyond the rainbow scattering angle; there remain the reflected rays. Their effects can be neglected as well in the extremely backward angular region at sufficiently high energy. In order to control that this latter approximation is correct, we must assume that the edge of the interaction region is not sharp, as in our primitive model, but we must suppose more realistically that its surface has a certain diffuseness. Then one can evaluate the contribution of the reflected component (see, e.g., [12]) and one can easily check that it is decreasing as the surface diffuseness and the bombarding energy are increasing.

It remains to spend a few words on the effects of the Coulomb field. First of all we neglect the Coulomb trajectories [trajectories belonging to class (i)] by subtracting the Rutherford amplitude; nevertheless, the Coulomb field acts also on the other classes of trajectories, in particular, the grazing ones. The first modification is due to the fact that now the incident rays are not straight lines parallel to the axis of the target, and accordingly the grazing angles change, depending on the Sommerfeld parameter $\eta = \mu Z_1 Z_2 e^2 / k (\hbar = 1)$, which tends to zero as $k \rightarrow \infty$. Therefore, at energy sufficiently high, these modifications can be neglected again (see also [15]). At this point we can try a fit of the backward differential cross section, at fixed energy, by a formula of the following type:

$$\left(\frac{d\sigma}{d\Omega}\right) \approx C |P_\lambda(-\cos\theta)|^2. \quad (32)$$

Here we take the constant C equal to 1 [recall that $P_\lambda(-\cos\pi) = 1$]. Then we fit the dimensionless differential cross section, measured by Delbar *et al.* [19], with the formula $|P_\lambda(-\cos\theta)|^2$. The fits at three different values of the energy, in the neighborhood of $E_{c.m.} = 45$ MeV are shown in

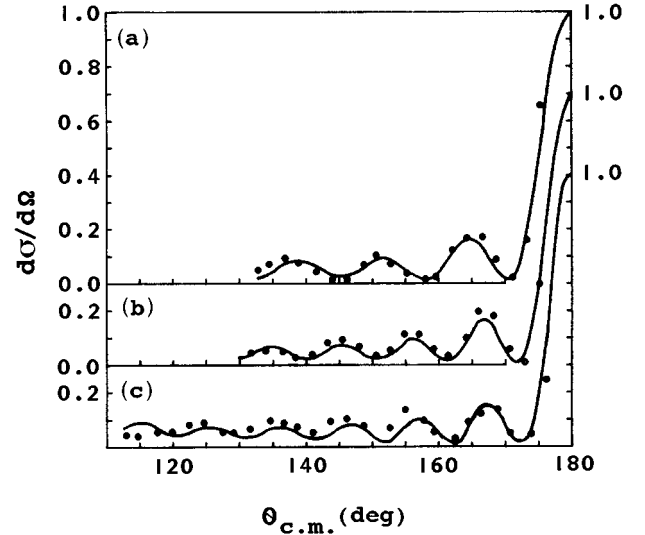


FIG. 5. Elastic scattering angular distribution for the α - ^{40}Ca system. The continuous line represents the dimensionless normalized cross section $(d\sigma/d\Omega) = |P_\lambda(-\cos\theta)|^2$, the solid circles denote the observed data σ/σ_R taken from [19]; (a) $E_{c.m.} = 37.8$ MeV, (b) $E_{c.m.} = 45$ MeV, (c) $E_{c.m.} = 48.6$ MeV.

Fig. 5. The reason of this particular choice of the energy is motivated by the fact that at lower energy the interference with the reflected rays cannot be neglected and it obscures the effect of the surface waves even backwards. On the contrary, in the fits reported in Fig. 5, the accord with the experimental data is satisfactory in a wide angular range. Consequently the values of the two fitting parameters $\alpha \equiv \text{Re}\lambda$ and $\beta \equiv \text{Im}\lambda$ can be taken with good confidence and they are reported in Table III (second and third columns, respectively). In the same table these values of β are compared with those (reported in the fourth column) obtained evaluating β by the use of formula (29) putting $\gamma = 0.1$ (MeV) $^{-1/2}$ (which is the numerical value obtained by the fit of the phase shifts with odd angular momentum).

Finally let us note that we fit the differential cross section measured by Delbar *et al.* [i.e., $\sigma(\theta)/\sigma_R(\theta)$, $\sigma_R(\theta) = \text{Rutherford cross section}$] by the use of formula (32). This amounts to neglecting the factor $[\sin^4(\theta/2)]^{-1}$. This approximation, however, is legitimate in the extremely backward angular region which is the domain of interest for our analysis.

We can conclude that the agreement between the values obtained by fitting the backward cross section at high energy

TABLE III. Values of the complex angular momentum ($\alpha + i\beta$) determined by formula (32) (second and third columns); values of β obtained by formula (29), putting $\gamma = 0.1$ (MeV) $^{-1/2}$ (fourth column).

$E_{c.m.}$ MeV	α	β	β
	Surface waves	Surface waves	Resonances
37.8	13.7	0.61	0.61
45	16.6	0.7	0.67
48.6	16.9	0.78	0.69

(surface waves), and those obtained by extrapolating the fits of the resonances is satisfactory see Table III.

C. Remarks and conclusions

The main results of our paper are the following.

(1) The theoretical analysis and the phenomenological evidence of two trajectories of Regge poles which interpolate two rotational sequences of resonances, respectively, of even and odd parity.

(2) The representations of the phase shifts given by formulas (17) and (18), which take into account the effects of the repulsive forces due to the Pauli exchange effects and to the hard core. The interpolation of resonances [point (1)] is realized by the use of formulas (17) and (18).

(3) The theoretical and phenomenological proof that these poles, extrapolated to high energies (see, in particular, Table III) give rise to surface waves emerging in the diffractive backward peaks.

In connection with point (3) some remarks are, however, necessary.

(i) In order to obtain a pictorial representation of the surface waves we have used a simplified model of the interaction region, at high energies, represented by a weakly absorbing sphere with a thin transparent border. This model allows us to derive easily a picture of the waves creeping around the target [see formula (25)] and to describe qualitatively the phenomena. Let us, however, remark that a sharp edge of the interaction region is not realistic, as we have already noted in connection with the evaluation of the contribution of the reflected rays. This model corresponds, in fact, to a potential of compact support which represents a too drastic approximation, and it cannot be used for fitting the experimental data. In the older analyses the form of the optical potential chosen was generally of the Woods-Saxon type; more recently many modifications have been proposed, like to take a Woods-Saxon squared form factor [20], or to introduce an angular-momentum-dependent absorption [21]. Furthermore, let us recall that within the optical-potential framework some models for explaining the surface waves have been proposed, like the model of Brink *et al.* [22], which is particularly refined. At this point, however, we must distinguish between a model, useful for obtaining a qualita-

tive description of the phenomena, and the class of potentials admitting a representation of the scattering amplitude in terms of poles in the complex angular-momentum plane. As we have seen in Sec. II, the class of potentials admitting a Watson resummation leading to a Regge representation of type (1) is limited to the Yukawian class and therefore it is rather restricted. In particular, the potentials of compact support as well as the Woods-Saxon potentials do not belong to this class [23]. But if we limit ourselves to consider a parametrization, and accordingly an approximation of the scattering amplitude in terms of poles in the complex angular-momentum plane, without pretending that the background integral runs along a parallel to the imaginary axis, as in formula (1), then the class of admitted potentials is much larger including more realistic prototypes. Following Tamura and Wolter [23] we note that in low-energy physics the complex angular-momentum parametrizations may in general be regarded as a method to separate the dominant pole contribution from a smooth background term. From these considerations it follows that the validity of our approximation, and in particular the fitting formula (32), is not restricted to the simplified model illustrated in Sec. II C, but it can be justified in a larger and more realistic class of potentials.

(ii) The data of Delbar *et al.* [19] show in a very clear way the three fundamental phenomena present in the α - ^{40}Ca elastic scattering in the energy range between 35 and 60 MeV (in the Laboratory system): (α) forward diffractive peaks, (β) rainbow dips, (γ) backward diffractive peaks and ALAS. We have only considered the last one (of the three phenomena indicated above), since it can be directly related to the rotational resonances as shown by Fig. 5 and Table III. Accordingly we have fitted the differential cross section in an angular region beyond the rainbow dips. Let us, however, mention that the data of Delbar *et al.* present spectacular examples of nuclear rainbows (as we have already noted), particularly evident at 49.5 MeV (in the laboratory system). These rainbows prove, without any ambiguity, that the absorption in the interaction region is weak. The rainbows are, in fact, generated by the refracted rays which penetrate the interaction region without being absorbed. In spite of the great relevance of these effects, we do not treat these phenomena in the present paper, and the interested reader is referred to [16–18].

-
- [1] A. Sommerfeld, *Partial Differential Equations in Physics* (Academic Press, New York, 1964).
- [2] B. R. Levy and J. B. Keller, *Commun. Pure Appl. Math.* **12**, 159 (1959).
- [3] D. Ludwig, *Commun. Pure Appl. Math.* **29**, 215 (1966).
- [4] V. De Alfaro and T. Regge, *Potential Scattering* (North-Holland, Amsterdam, 1965).
- [5] K. W. McVoy, *Ann. Phys. (N.Y.)* **43**, 91 (1967).
- [6] G. A. Viano, *Phys. Rev. C* **36**, 933 (1987).
- [7] G. A. Viano, *Phys. Rev. C* **37**, 1660 (1988).
- [8] S. Okai and S. C. Park, *Phys. Rev.* **145**, 787 (1966).
- [9] H. M. Nussenzveig, *Ann. Phys. (N.Y.)* **34**, 23 (1965).
- [10] W. Durso and P. Signell, *J. Math. Phys. (N.Y.)* **5**, 350 (1964).
- [11] A. Erdelyi, W. Magnus, F. Oberhettinger, and F.G. Tricomi, *Higher Transcendental Functions* (McGraw-Hill, New York, 1953), Vol. 1.
- [12] D. M. Brink, *Semiclassical Methods for Nucleus-Nucleus Scattering* (Cambridge University Press, Cambridge, England, 1985).
- [13] K. Langanke, *Nucl. Phys.* **A377**, 53 (1982).
- [14] M. H. Nussenzveig, *J. Math. Phys. (N.Y.)* **10**, 82 (1969); **10**, 125 (1969).
- [15] E. Di Salvo and G. A. Viano, *Nuovo Cimento A* **71**, 261 (1982).
- [16] H. M. Khalil, K. W. McVoy, and M. M. Shalaby, *Nucl. Phys.* **A455**, 110 (1986).
- [17] K. W. McVoy, H. M. Khalil, M. M. Shalaby, and G. R. Satchler, *Nucl. Phys.* **A455**, 118 (1986).

- [18] K. W. McVoy, Nucl. Phys. **A455**, 141 (1986).
- [19] Th. Delbar, Gh. Grègoire, G. Paic, R. Ceuleneer, F. Michel, R. Vanderpoorten, A. Budzanowski, L. Friendl, K. Grotowski, S. Micek, R. Planeta, A. Strzalkowski, and K. A. Eherhard, Phys. Rev. C **18**, 1237 (1978).
- [20] F. Michel and R. Vanderpoorten, Phys. Rev. C **16**, 142 (1977).
- [21] K. A. Eberhard, Phys. Lett. **33B**, 343 (1970).
- [22] D. M. Brink and N. Takigawa, Nucl. Phys. **A279**, 159 (1977).
- [23] T. Tamura and H. H. Wolter, Phys. Rev. C **6**, 1976 (1972).